

Infrared extrapolations for atomic nuclei

R. J. Furnstahl¹, G. Hagen^{2,3}, T. Papenbrock^{3,2}, and
K. A. Wendt^{3,2}

¹Department of Physics, The Ohio State University, Columbus, OH 43210

²Physics Division, Oak Ridge National Laboratory, Oak Ridge, TN 37831 USA

³Department of Physics and Astronomy, University of Tennessee, Knoxville, TN 37996, USA

E-mail: furnstahl.1@osu.edu, hagen@ornl.gov, tpapenbr@utk.edu,
kwendt2@utk.edu

Abstract. Harmonic oscillator model-space truncations introduce systematic errors to the calculation of binding energies and other observables. We identify the relevant infrared scaling variable and give values for this nucleus-dependent quantity. We consider isotopes of oxygen computed with the coupled-cluster method from chiral nucleon-nucleon interactions at next-to-next-to-leading order and show that the infrared component of the error is sufficiently understood to permit controlled extrapolations. By employing oscillator spaces with relatively large frequencies, well above the energy minimum, the ultraviolet corrections can be suppressed while infrared extrapolations over tens of MeVs are accurate for ground-state energies. However, robust uncertainty quantification for extrapolated quantities that fully accounts for systematic errors is not yet developed.

PACS numbers: 21.10.Dr, 21.60.-n, 31.15.Dv, 21.30.-x

Submitted to: *J. Phys. G: Nucl. Phys.*

1. Introduction

Wave-function based methods for computing atomic nuclei, such as exact diagonalization [1, 2], coupled cluster [3, 4, 5], self-consistent Green's functions [6], or in-medium similarity renormalization group (SRG) [7, 8], require a computational effort that depends strongly on the size of the Hilbert space used. Truncating this model space introduces systematic errors that must be quantitatively analyzed for a given Hamiltonian and nucleus. By understanding these errors, we can devise controlled extrapolation techniques for energies and other observables.

Though we deal with a quantum mechanical problem, it is most instructive to look first at classical phase space. Let us consider the deuteron wave function, calculated from a realistic two-body interaction, and compute its Wigner transform. We recall that the Wigner transform

$$f(\mathbf{r}, \mathbf{p}) = \int d^3\mathbf{k} \frac{e^{i\mathbf{r}\cdot\mathbf{k}}}{(2\pi)^3} \psi^*(\mathbf{p} + \mathbf{k}/2) \psi(\mathbf{p} - \mathbf{k}/2), \quad (1)$$

is a mapping of a wave function to a phase-space distribution. Figure 1 shows the results for chiral effective field theory (EFT) Hamiltonians [9] with two different cutoffs. We see that the dominant part of the Wigner transform extends in (radial) position essentially up to the deuteron radius (though the exponential tail casts a long shadow), and in momentum space up to the cutoff of the interaction.

Generalizing this result, the number of single-particle states required to compute a nucleus with radius R from an interaction with cutoff Λ is essentially given by

$$n = \frac{1}{(2\pi)^3} \int d^3r \int d^3p \propto (R\Lambda)^3. \quad (2)$$

Here, we have not counted spin/isospin degrees of freedom. The key result is that the number of single-particle states grows as the third power of the cutoff, and it is proportional to $R^3 \propto A$ for a nucleus with mass number A . The proportionality constant in Eq. (2) depends on the actual basis one uses, and some efficiencies can possibly be gained from abandoning the oscillator basis in favor of Berggren bases [10], Sturmian bases [11] or discrete variable representations [12]. Equation (2) also makes clear that halo nuclei can be as expensive to compute as much heavier nuclei, and that much is to be gained by lowering the cutoff Λ of the interaction. This latter point explains why low-momentum interactions (e.g. $V_{\text{low } k}$ [13] or SRG [14]) are so popular.

When working with the harmonic-oscillator basis, its extent in position and momentum space must exceed the radius of the nucleus and the cutoff of the interaction, respectively. In other words, one must choose the oscillator frequency and the maximum excitation energy such that the ellipsoidal phase-space area of the oscillator covers the relevant parts of the Wigner function for the nucleus. Let $b = \hbar/\sqrt{m\hbar\Omega}$ denote the oscillator length, where m is the nucleon mass. Then a simple semiclassical argument implies that for an oscillator basis with up to N excited quanta, we must demand

$$\sqrt{2N} \geq R/b \quad \text{and} \quad \sqrt{2N} \geq \Lambda b. \quad (3)$$

The ellipses corresponding to equality signs in these expressions are also shown in Fig. 1. We see that only the tails of the Wigner function – both in the directions of position and momentum – extend beyond the ellipses. Let us also note that Fig. 1 serves mainly as an illustration but should not be used for quantitative conclusions. Only in the semiclassical limit is it possible to quantitatively relate Wigner functions to classical phase-space structures [15]. The questions to address are what error results from the omission of these tails for the binding energy and other observables in a finite oscillator basis, and how quickly do these quantities converge as the number of basis states is increased?

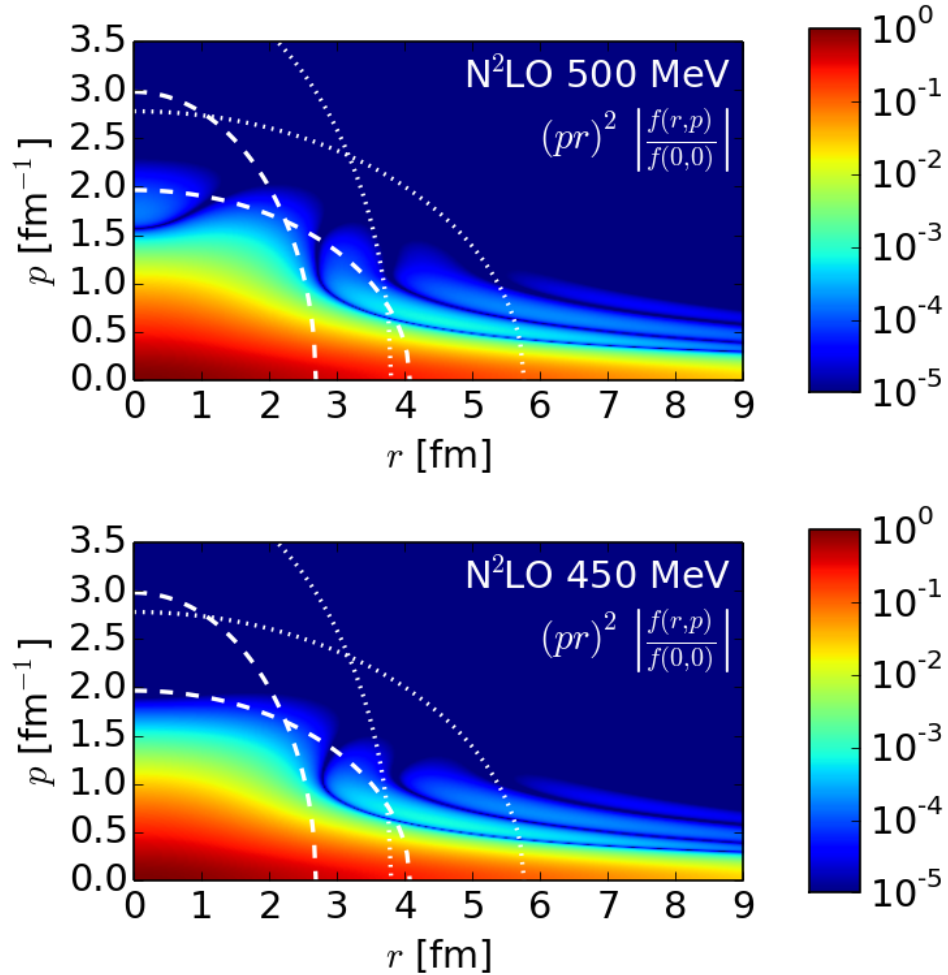


Figure 1. (Color online) Top: “s-wave” projection of Wigner function from deuteron wave function for a chiral N²LO potential with a regulator cutoff of $\Lambda_{UV} = 500$ MeV. Abscissa is r in units of fm, ordinate is momentum p in units of fm⁻¹. The dashed lines are semi-classical harmonic oscillator cutoffs for $N = 4$ and two different oscillator frequencies ($\hbar\Omega = 20$ and 50 MeV). The dotted lines are the same with $N = 8$. Bottom: same as top but for a lower regulator cutoff $\Lambda_{UV} = 450$ MeV.

2. Infrared cutoffs of the oscillator basis

The semi-classical estimates (3) are a useful guide, but for practical purposes we have to understand how the infrared (IR) cutoff $\Lambda_{\text{IR}} \equiv \pi/L$ and ultraviolet (UV) cutoff Λ_{UV} of a finite oscillator basis can become tools for the extrapolation of observables. The leading-order estimates for these cutoffs are based on $L \approx \sqrt{2Nb}$ and $\Lambda_{\text{UV}} \approx \sqrt{2N}/b$, respectively [16, 17, 18]. Clearly, L and Λ_{UV} are semiclassical estimates for the extent of the oscillator basis in position and momentum space, respectively.

The nucleon-nucleon forces (and many-body forces) used for wave-function based methods, such as chiral effective field theory (EFT) or low-momentum interactions, all have momentum-space regulators that rapidly drive them to zero above a cutoff Λ . If Λ_{UV} is less than or comparable to Λ , the UV corrections to the energy and other observables will depend on the details of the regulators (but less on the nucleus under consideration). But when Λ_{UV} sufficiently exceeds Λ (see Sec. 4), rapid UV convergence is observed in practical calculations, so that UV extrapolations are not needed.

In this paper, we focus solely on IR extrapolations. We note that the long wavelength structure of a bound state stems from its exponential fall-off in position space and is independent of the details of the interaction. A finite extent of the oscillator basis in position space cuts off this exponential tail and thereby yields an energy correction. References [19, 20, 21] provide a theoretical basis for IR extrapolations. It is established in these papers that a finite oscillator basis with N excited quanta and oscillator length b is, at low momenta, indistinguishable from a box of size

$$L_2(N, \hbar\Omega) \approx \sqrt{2(N + 3/2 + 2)b} . \quad (4)$$

Here, the approximate sign indicates that this is the next-to-leading order approximation of the box size in the limit of $N \gg 1$. This result can be derived from the fact that $\Lambda_{\text{IR}}^2 \equiv (\pi/L_2)^2$ is the lowest eigenvalue of the momentum operator squared in the finite oscillator basis [20]. A single-particle wave function of an s -wave bound state, approximated in a finite oscillator basis, only differs by high-momentum components from the same wave function approximated in a spherical well of radius L_2 . For a partial wave with angular momentum l , one has $N = 2n + l$ in Eq. (4). Thus, for fixed oscillator spacing $\hbar\Omega$ the length $L_2(N, \hbar\Omega)$ is a staircase function that increases at even (odd) values of N for even (odd) values of l .

This knowledge can be used to understand the IR extrapolations of bound states. The equivalent finite size L_2 of the oscillator basis has the effect on a position-space bound state of enforcing that the wave function has a node at L_2 . This correction to the true bound-state wave function is a long-wavelength phenomenon and can thus be understood in model-independent ways [20, 21]. The leading-order IR extrapolation formula for an s -wave bound-state energy of a single-particle system is

$$E(L_2) = E_\infty + \frac{\hbar^2 k_\infty^2 \gamma_\infty^2}{\mu} \exp(-2k_\infty L_2) . \quad (5)$$

Here, k_∞ is the bound-state momentum, i.e. $E_\infty = \hbar^2 k_\infty^2 / (2\mu)$ is the bound-state energy, μ is the reduced mass, and γ_∞ is the asymptotic normalization constant. Higher-order

corrections, which are suppressed by powers of $\exp(-2k_\infty L_2)$, and extensions to general orbital angular momentum are also known [21].

Although the IR extrapolation formula (5) was derived for a single-particle degree of freedom (or systems that can be reduced to such), it has also been applied to bound states of many-body problems [19, 22, 23, 24, 25, 26] via

$$E(L) = E_\infty + A_\infty \exp(-2k_\infty L), \quad (6)$$

with $L(N, \hbar\Omega)$ still to be specified. The idea is that k_∞ can be generally interpreted as the (least) separation energy for the nucleus under consideration, so that (6) follows from the two-body derivation in Ref. [21] but now using the S matrix for the corresponding break-up reaction. Because of the many approximations involved, A_∞ , E_∞ , and k_∞ are all treated as fit parameters. To apply the extrapolation formula (6), one needs to work with bound states (i.e. the fully converged energy needs to be negative), L must exceed the radial extent of the nucleus under consideration, and the UV cutoff Λ_{UV} must be sufficiently greater than the cutoff of the interaction. In practice, one can calculate using large values of $\hbar\Omega$ to ensure that UV corrections are much smaller than the IR corrections.

Let us consider applying Eq. (6) to compute the ground-state energies of oxygen isotopes. As a first step, we plot the energies obtained using different model spaces as a function of the effective box size L . The top panels in Fig. 2 show the results for ^{16}O (left) and ^{24}O (right) when plotted versus $L = L_2$. The data points stem from model spaces with $N = 8, 10, 12$ oscillator quanta and $\Lambda_{UV} > 750$ MeV, so that UV corrections are presumably small. Clearly, the data points do not fall on a single line for either nucleus, and similar results are found for ^{22}O . Earlier studies [20] showed that the smoothness of $E(L)$, when plotted for a large set of N and $\hbar\Omega$ values for which UV corrections are small, is a sensitive diagnostic of the quality of $L(N, \hbar\Omega)$. Thus, $L = L_2$ is not the accurate box size of the harmonic oscillator basis for fermionic many-body systems. In the next section we derive a more accurate value L_{eff} by revisiting the underlying basis for the effective box size. As we will see, this value depends on the nucleus under consideration.

3. Box size $L_{\text{eff}}(N, \hbar\Omega)$ for nuclei

The paradigm for IR extrapolations in the harmonic oscillator basis can be stated as follows: *For sufficiently low energies (and long wavelengths), a finite oscillator basis is indistinguishable (in the sense of an effective theory) from a spherical box with an appropriately chosen radius.* This radius is determined by matching the lowest (most infrared) eigenvalue of the squared momentum operator in the oscillator basis to the lowest value in the box. To apply this matching procedure to the many-body case, we have to consider the lowest *total* squared momentum $\sum_{i=1}^A p_i^2$ for a given nucleus. To do so, we identify the occupation numbers ν_{nl} that give the lowest kinetic energy for that nucleus, and then equate the eigenvalue of the total squared momentum operator

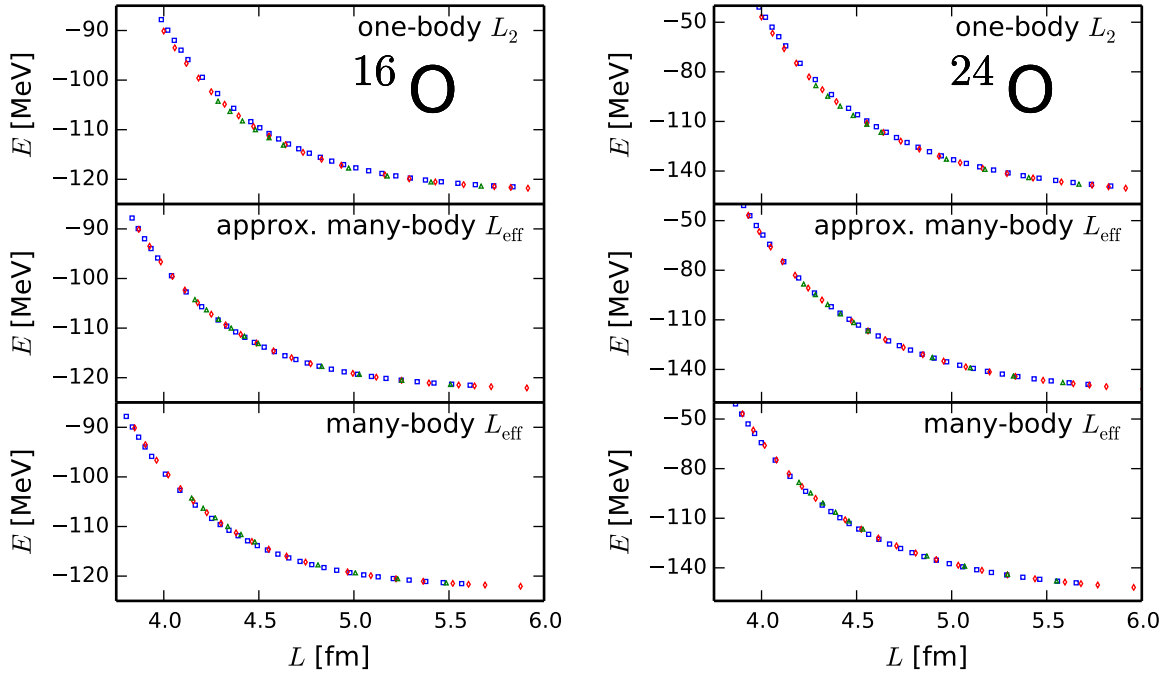


Figure 2. Ground-state energies versus the scaling variable L from coupled-cluster theory in the CCSD approximation for ^{16}O (left) and ^{24}O (right) using a chiral N^2LO potential with a regulator cutoff of $\Lambda_{\text{UV}} = 500 \text{ MeV}$. The squares, diamonds and triangles stem from model spaces with $N = 8, 10, 12$, respectively. The top panels use the naive single-particle choice $L = L_2(N, \hbar\Omega)$, while the middle and bottom panels use approximate and exact $L = L_{\text{eff}}(N, \hbar\Omega)$, respectively, as described in Sec. 3.

for the oscillator basis to the total squared momentum for the same number of nucleons (occupying identical partial waves) in a spherical box of size L_{eff} , i.e.

$$\sum_{nl} \nu_{nl} \kappa_{ln}^2 = \sum_{nl} \nu_{nl} \left(\frac{a_{l,n}}{L_{\text{eff}}} \right)^2. \quad (7)$$

Here, κ_{ln}^2 is the eigenvalue of the single-particle squared momentum operator and $a_{l,n}$ is the $(n+1)^{\text{th}}$ zero of the spherical Bessel function j_l [27]. This yields

$$L_{\text{eff}} = \left(\frac{\sum_{nl} \nu_{nl} a_{l,n}^2}{\sum_{nl} \nu_{nl} \kappa_{ln}^2} \right)^{1/2}. \quad (8)$$

We can parameterize this result using L_2 by introducing N_{eff} , which is defined as a function of N by

$$L_{\text{eff}}(N, \hbar\Omega) \equiv L_2(N_{\text{eff}}, \hbar\Omega). \quad (9)$$

We note that the approach to the many-body scaling variable L_{eff} can be extended to any localized basis set by numerically computing the eigenvalues of the total squared momentum operator and equating them to the corresponding eigenvalues of a spherical box with radius L_{eff} .

For an understanding of L_{eff} (or N_{eff}), it is useful to consider analytical approximations to L_{eff} . These are based on approximate expressions for the eigenvalues κ_{lm} which are valid for model spaces with $N \gg 1$. In the single-particle problem (or the deuteron in its center-of-mass frame), the $(m+1)^{\text{th}}$ eigenvalue κ_{lm}^2 in a harmonic-oscillator model space with up to N quanta of excitation is given to good approximation [21] by

$$\kappa_{lm}^2 \approx \frac{a_{l,m}^2}{2(N_l + 3/2 + 2)b^2} = \frac{a_{l,m}^2}{(L_2(N, \hbar\Omega))^2}, \quad (10)$$

and

$$N_l = \begin{cases} N, & \text{for } N \text{ and } l \text{ even or for } N \text{ and } l \text{ odd;} \\ N-1, & \text{for } N \text{ even and } l \text{ odd or for } N \text{ odd and } l \text{ even.} \end{cases} \quad (11)$$

As a check, consider a single particle in a model space with $N = 2n + l$. We equate the lowest eigenvalue κ_{l0}^2 to the lowest eigenvalue $(a_{l,0}/L)^2$ in a spherical box of radius L for angular momentum l . This yields $L = L_2(N, \hbar\Omega)$ as defined in Eq. (4).

Thus, approximate values for L_{eff} are found by inserting the analytical approximations (10) into Eq. (8). The middle panels of Fig. 2 show the ground-state energies for $^{16,24}\text{O}$ when plotted as a function of this approximate value for L_{eff} . Compared to the top panel ($L = L_2$), the improvement is considerable and clearly visible. The bottom panels of Fig. 2 show the ground-state energies for $^{16,24}\text{O}$ when plotted as a function of the exact numerical value for L_{eff} . Again, the data points fall close to a single line. For reasons we do not yet understand, the approximate L_{eff} (middle panel) leads to the smoothest line in ^{16}O , while the exact L_{eff} yields the smoothest line in ^{24}O .

Table 1 gives N_{eff} for isotopes $^{12,14}\text{C}$ and $^{16,22,24}\text{O}$. These results are determined by diagonalizing the operator $\sum_{i=1}^A p_i^2$ in the specified model space. We note that the “square” model space (defined by each particle allowed up to N oscillator quanta) is used in the coupled-cluster calculations of this paper and by other methods [6, 7, 8]. This model space differs from the “triangular” full $N\hbar\Omega$ model space used in most NCSM calculations.

Let us make some comments on the values of N_{eff} in Table 1. We recall that N_{eff} is computed from the exact eigenvalues κ_{lm}^2 of the total squared momentum operator. The resulting values for N_{eff} are a few percent smaller than the results one obtains from using the $N \gg 1$ approximation (10) in the computation of N_{max} . However, these latter approximations $N_{\text{eff}}^{\text{approx}}$ can be understood semi-quantitatively as follows. For the nucleus ^4He (not shown) we have $N_{\text{eff}}^{\text{approx}} = N$ ($N_{\text{eff}}^{\text{approx}} = N - 1$) for even (odd) N because only s -waves are occupied, so $L_2(N, \hbar\Omega) = L_{\text{eff}}(N, \hbar\Omega)$. For $^{12,14}\text{C}$ and ^{16}O , p -waves are at the Fermi surface, and for pure p -waves and even (odd) N one has $N_{\text{eff}}^{\text{approx}} = N - 1$ ($N_{\text{eff}}^{\text{approx}} = N$), see Eq. (10). Thus, our values for $N_{\text{eff}}^{\text{approx}}$ are closest to these extreme values for ^{16}O and somewhat farther away for $^{14,12}\text{C}$. For $^{22,24}\text{O}$, d -shell orbitals are at the Fermi surface for the kinetic energy, countering the effects from the lower-lying p waves and effectively increasing (decreasing) $N_{\text{eff}}^{\text{approx}}$ for even (odd) N . As

N	^{12}C	^{14}C	N_{eff} ^{16}O	^{22}O	^{24}O
1	0.365	0.393	0.413	—	—
2	0.745	0.709	0.684	0.899	0.939
3	2.515	2.545	2.566	1.939	1.844
4	2.902	2.867	2.842	3.092	3.137
5	4.586	4.617	4.639	4.116	4.033
6	4.976	4.941	4.917	5.187	5.236
7	6.629	6.660	6.682	6.205	6.127
8	7.020	6.985	6.961	7.245	7.296
9	8.658	8.689	8.711	8.259	8.185
10	9.049	9.015	8.990	9.285	9.337
11	10.678	10.709	10.732	10.297	10.225
12	11.070	11.036	11.011	11.313	11.366
13	12.693	12.725	12.748	12.324	12.254
14	13.085	13.051	13.027	13.335	13.389
15	14.705	14.737	14.760	14.345	14.276
16	15.097	15.064	15.040	15.352	15.406
17	16.715	16.747	16.770	16.361	16.293
18	17.107	17.074	17.050	17.366	17.421
19	18.723	18.755	18.778	18.375	18.307
20	19.115	19.082	19.058	19.377	19.433

Table 1. Effective excitation number N_{eff} for isotopes $^{12,14}\text{C}$ and $^{16,22,24}\text{O}$, computed from the exact eigenvalues of the total squared momentum operator. Where no result is given, the model space is too small to accommodate A nucleons.

naively expected, the effect is larger in ^{24}O than in ^{22}O . From these arguments, one expects $N - 1 \leq N_{\text{eff}}^{\text{approx}} \leq N$ in general.

We note that the defect $N - N_{\text{eff}}$ varies very little (focusing on either even or odd N) as N varies. In practice, one might thus take a fixed defect (say from $N = 10$ or so) and consider the small variation of the defect a higher-order correction. We also note an odd-even staggering of N_{eff} . This staggering is caused by Eq. (11) and has its root in the fact that L_2 increases for even (odd) values of angular momentum only at even (odd) values of N . In most NCSM and coupled-cluster calculations, practitioners limit themselves to sequences of model spaces with either even or odd values of N .

4. Extrapolations and the coupled-cluster method

In this section, we apply IR extrapolations to the results of the coupled-cluster method with singles and doubles (CCSD) calculations [3, 4, 28, 5]. Our interest is twofold. First, we want to study in more detail whether L_{eff} is also the relevant length scale when

approximate many-body solutions (such as CCSD) are employed. We note that most *ab initio* methods that presently compute nuclei beyond the p shell employ approximate solutions of the many-body problem [29, 30, 7, 25, 24]. Second, we want to probe the extrapolation formula (6) over a large energy range and see how large the model space needs to be for a reliable and accurate extrapolation.

We compute the ground-state energies of the nuclei $^{16,22,24}\text{O}$ using the next-to-next-to-leading order chiral nucleon-nucleon interaction of Ref. [9] with a cutoff $\Lambda_\chi = 500$ MeV. This interaction has been optimized to scattering data of the nucleon-nucleon system and deuteron bound-state properties. It is similar in quality to the chiral nucleon-nucleon interaction NNLO_{opt} [31], which was optimized with respect to phase shifts.

Figure 3 shows the CCSD ground state energies for ^{16}O as a function of L_{eff} (left figure) and $\hbar\Omega$ (right figure) for model spaces with $N = 8, 10, 12$. Our model spaces have oscillator frequencies in the interval $\hbar\Omega/(\text{MeV}) \in [16, 70]$. At fixed N , the energy computed at the highest oscillator frequency corresponds to the smallest value of L_{eff} and exhibits the smallest UV error. In the left panel of Fig. 3 the solid data points forming the exponential envelope have negligible UV corrections and can be used in the IR extrapolation. As seen in the right panel, these frequencies are much larger than the naive estimate $\hbar\Omega_{\text{min}} \approx \hbar^2\Lambda_\chi/(mR)$ that minimizes the energy for a nucleus of radius R and interaction with cutoff Λ_χ [17]. The exponential extrapolation (6) to all solid data points is shown as a dashed line, and the asymptote E_∞ as a full line.

The extrapolation results are from a least-squares penalty-function fit with equal weighting [32] of the parameters E_∞ , k_∞ , and A_∞ . We note that the exponential extrapolation practically works over the entire range of about 60 MeV. While the energy correction can be a substantial fraction of the total binding energy, we have $\exp(-2k_\infty L_{\text{eff}}) \ll 1$ over the considered range of L_{eff} . For fixed N , the (very small) UV corrections are expected to increase with increasing L_{eff} , see Fig. 20 of Ref. [20] as an example. We note that all solid data points employed in the IR extrapolation in Fig. 3 are from model spaces with $\Lambda_{\text{UV}} > 750$ MeV. The UV cutoff parameter of the nucleon-nucleon interaction used here is $\Lambda_\chi \approx 500$ MeV, but this is not a sharp cutoff, which is why Λ_{UV} must be sufficiently higher than Λ_χ so that effects from the omitted UV tail are small.

Let us discuss errors and error estimates. We applied a theory, derived for the deuteron and $k_\infty L_{\text{eff}} \gg 1$ to many-body systems and for $k_\infty L_{\text{eff}} > 4$ or so. We view the extrapolation formula (6) as a leading order and systematically improvable result applied to a complex nucleus over a wide range of $k_\infty L_{\text{eff}}$, neglecting higher-order corrections. We also deal with systematic errors from the CCSD approximation (recall that L_{eff} was worked out for an exact solution of the operator $\sum_{i=1}^A p_i^2$). We believe that UV errors are negligible. Thus, we have systematic errors from neglected corrections in the IR and from the approximate many-body method. Both systematic errors are hard to quantify. Some aspects of these systematic errors behave as statistical errors. For instance, we deal with a relatively small scatter of our data points around the exponential extrapolation. These

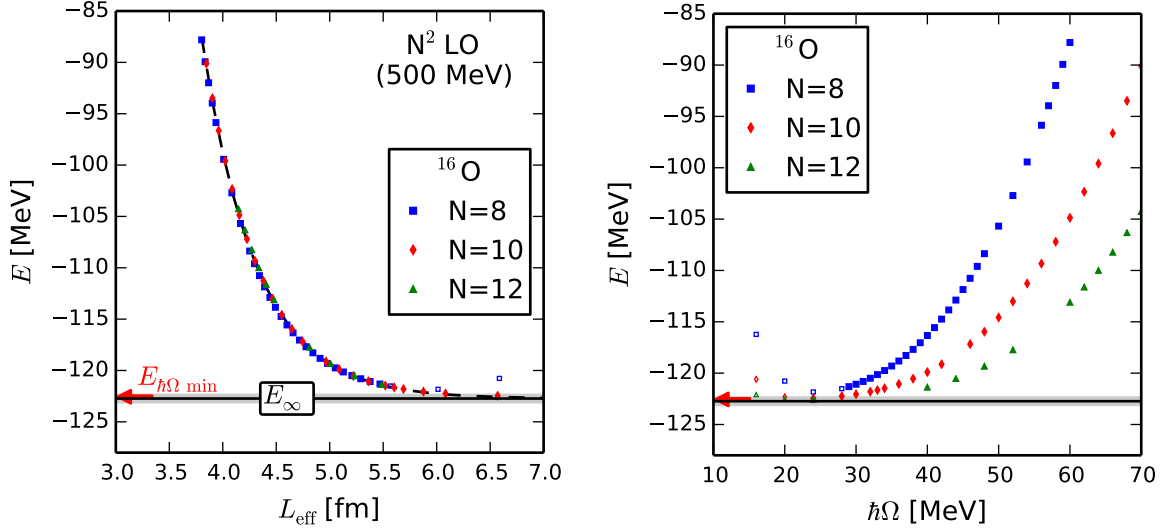


Figure 3. Ground-state energies in CCSD approximation for ^{16}O as a function of L_{eff} (left panel) and $\hbar\Omega$ (right panel) for harmonic-oscillator spaces with N as indicated. Dashed line: exponential fit of Eq. (5) to data with $N_{\text{max}} = 12$. Full line with band: asymptote E_{∞} from fit with 95% confidence interval. Hollow markers: points excluded from fit. The arrow marks the minimum energy $E_{\hbar\Omega \text{ min}}$ that is obtained when varying the oscillator spacing $\hbar\Omega$ for $N_{\text{max}} = 12$.

(relatively small) errors are easy to quantify and usually returned by fitting routines in the form of standard asymptotic errors computed from the covariance matrix. At this moment, these are the only errors we quantify and present in tables below. However, we emphasize that these errors are presumably much smaller than the systematic errors.

We fit Eq. (6) to ^{16}O , including increasingly larger sets of data points from model spaces with $N \leq N_{\text{max}}$. Table 2 shows the results. The error estimates are from the covariance matrix. We repeat that any systematic errors from sub-leading IR corrections or due to the CCSD approximation are not included. We note that the E_{∞} result for $N_{\text{max}} = 8$ is within the error estimates for $N_{\text{max}} = 10, 12$. Table 2 also shows the minimum energy $E_{\hbar\Omega \text{ min}}$ that is obtained at fixed N_{max} when varying the oscillator spacing $\hbar\Omega$. For the smaller model space with $N_{\text{max}} = 8$, the extrapolated energy E_{∞} is much closer to the “true” result (from extrapolations in larger model spaces) than the minimum energy $E_{\hbar\Omega \text{ min}}$, and this is the practical value of IR extrapolations. Of course, the challenge remains to give a meaningful error estimate for all model spaces.

The left panel of Fig. 4 shows a log plot of the difference $\Delta E = E - E_{\infty}$ for ^{16}O . The dashed line is the $N_{\text{max}} = 12$ exponential fit from Table 2. Deviations at the largest values of L_{eff} reflect UV corrections (open symbols are not used in the fit) and other systematic errors discussed above. However, the consistency of the fit to Eq. (6) over a large range of ΔE is striking. This suggests that there is enough information for reliable extrapolations even when using only calculations far from the energy minimum. This is validated for ^{16}O in the right panel of Fig. 4, where extrapolations are shown for

N_{\max}	8	10	12
$E_{\hbar\Omega_{\min}}$ [MeV]	-121.83	-122.46	-122.56
E_{∞} [MeV]	-122.62 ± 0.06	-122.68 ± 0.35	-122.73 ± 0.35
k_{∞} [fm $^{-1}$]	1.00 ± 0.00	0.99 ± 0.01	0.98 ± 0.01
A_{∞} [10^4 MeV]	6.95 ± 0.20	6.48 ± 0.49	5.96 ± 0.63

Table 2. Extrapolation parameters (and statistical error estimates) and energy minima for ^{16}O as a function of basis truncation N_{\max} . The neglected systematic errors are expected to dominate the error budget.

fixed $N = 8, 10$, and 12 using only points in each case with $\hbar\Omega \geq 50$ MeV. This plot can also be interpreted as showing that controlled and consistent (if not highly precise) extrapolations to $\hbar\Omega = 0$ (i.e. removing the IR cutoff for a fixed N) can be achieved if UV corrections are suppressed.

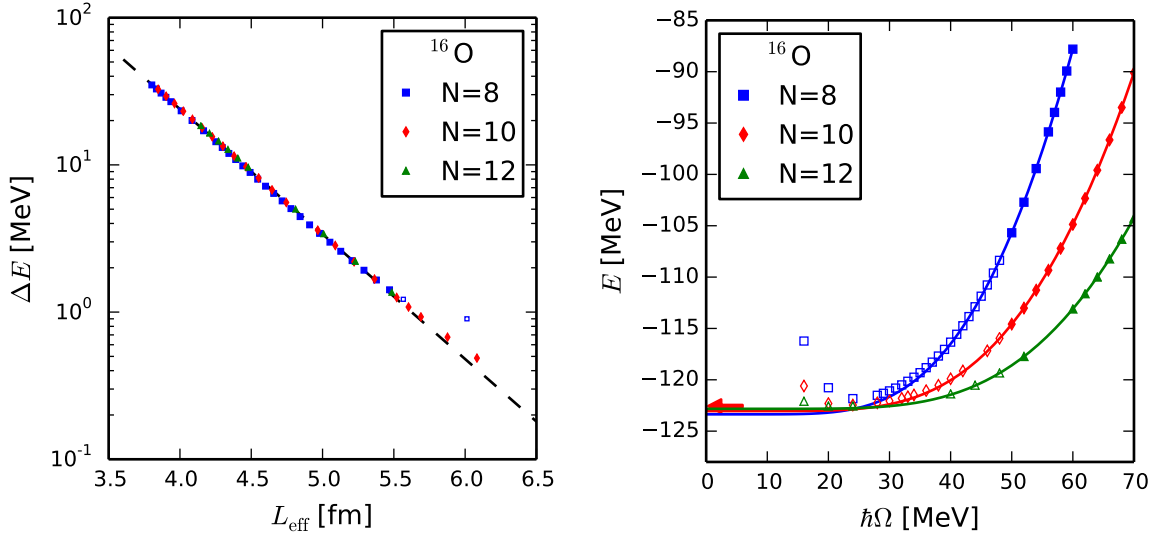


Figure 4. Left: energy difference ΔE for the ground-state energy (in CCSD approximation) of ^{16}O as a function of L_{eff} in a log plot. The symbols are as in Fig. 3, and the dashed line is the exponential fit for $N_{\max} = 12$ from Table 2. Right: ground-state energies as a function of $\hbar\Omega$ as in the right panel of Fig. 3. The solid lines are fits of Eq. (6) for fixed N to only the solid points. The arrow marks the minimum energy $E_{\hbar\Omega_{\min}}$ that is obtained when varying the oscillator spacing $\hbar\Omega$ for $N_{\max} = 12$.

Now we turn to the neutron-rich isotopes $^{22,24}\text{O}$. Figure 5 shows the CCSD ground-state energies for ^{22}O (left) and ^{24}O (right) as a function of L_{eff} . The exponential extrapolation (6), and the extrapolated ground-state energies $E_{\infty} = -148.41 \pm 0.60$ MeV (for ^{22}O) and $E_{\infty} = -155.38 \pm 0.83$ MeV (for ^{24}O) are also shown. These results employ model spaces with $N = 8, 10, 12$. Table 3 shows the extrapolated energies (and error estimates from the χ^2 fit) when only data points with $N \leq N_{\max}$ are employed in the

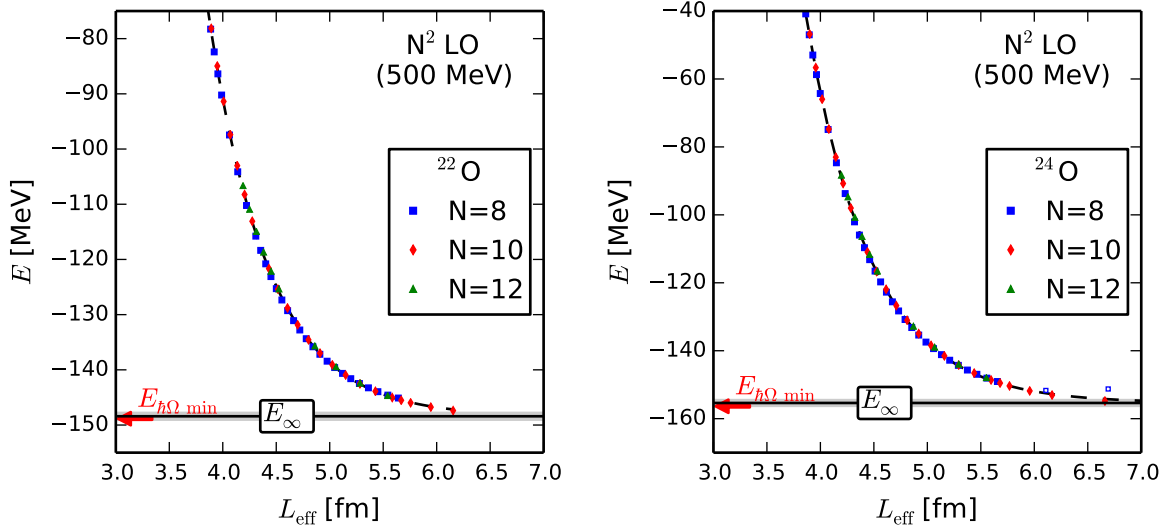


Figure 5. (Color online) Ground-state energies (CCSD approximation) for ^{22}O (left) and ^{24}O (right) as a function of L_2 for harmonic oscillator spaces with N as indicated. Dashed line: Exponential fit to Eq. (6). Full line with band: Asymptote E_∞ from errors from covariance matrix. Hollow markers: Points excluded from fit. The arrow marks the minimum energy $E_{h\Omega \min}$ that is obtained when varying the oscillator spacing $\hbar\Omega$ for $N_{\max} = 12$.

fit. We note that the fits work well over an energy range of tens of MeVs (see the left panels of Figs. 6 and 7). Again, the value of the IR extrapolation lies in the finding that $N_{\max} = 8$ extrapolations yield results that are close to the “true” ground-state energies (see the right panels of Figs. 6 and 7).

	N_{\max}	8	10	12
^{22}O	E_∞ [MeV]	-147.93 ± 0.01	-148.27 ± 0.47	-148.41 ± 0.60
	k_∞ [fm^{-1}]	0.91 ± 0.00	0.90 ± 0.01	0.89 ± 0.00
	A_∞ [10^4MeV]	8.56 ± 0.02	7.76 ± 0.52	7.19 ± 0.33
^{24}O	E_∞ [MeV]	-154.42 ± 0.10	-155.08 ± 0.63	-155.38 ± 0.83
	k_∞ [fm^{-1}]	0.83 ± 0.00	0.83 ± 0.01	0.82 ± 0.00
	A_∞ [10^4MeV]	7.89 ± 0.11	7.06 ± 0.52	6.53 ± 0.31

Table 3. Extrapolated energies E_∞ for $^{22,24}\text{O}$ as a function basis truncation N_{\max} . The energy minima for $^{22,24}\text{O}$ in a $N_{\max} = 12$ model-space are found at the oscillator frequency $\hbar\Omega = 20 \text{MeV}$ and are $E_{h\Omega \min} = -148.85 \text{MeV}$ and $E_{h\Omega \min} = -156.35 \text{MeV}$, respectively.

Our study shows that IR extrapolation can be a practical tool for approximate solutions of the nuclear many-body problem. The extrapolation is accurate and reliable over a large energy range of tens of MeV. For the employed chiral interaction at NNLO, the examples of $^{16,22,24}\text{O}$ suggest that ground-state energies of p -shell and sd -shell nuclei

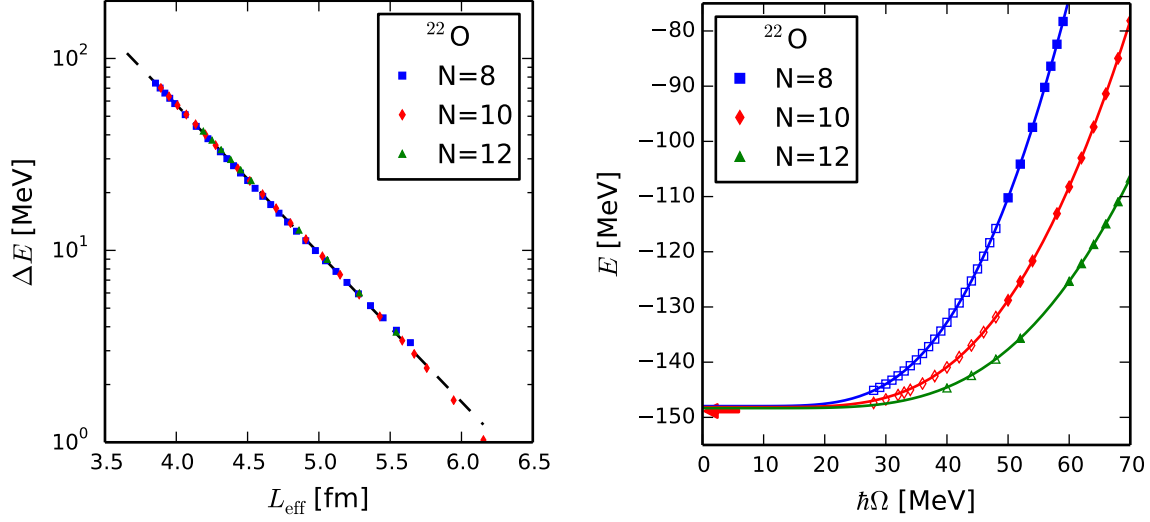


Figure 6. Left: energy difference ΔE for the ground-state energy (in CCSD approximation) of ^{16}O as a function of L_{eff} in a log plot. The symbols are as in Fig. 3, and the dashed line is the exponential fit for $N_{\text{max}} = 12$ from Table 3. Right: ground-state energies as a function of $\hbar\Omega$ as in the right panel of Fig. 3. The solid lines are fits of Eq. (6) for fixed N to only the solid points. The arrow marks the minimum energy $E_{\hbar\Omega \text{ min}}$ that is obtained when varying the oscillator spacing $\hbar\Omega$ for $N_{\text{max}} = 12$.

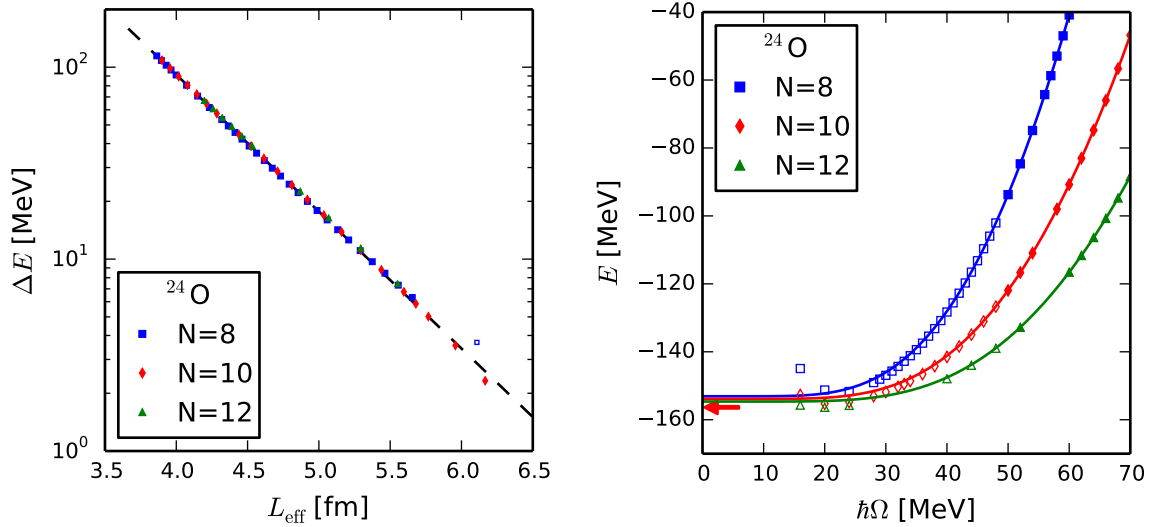


Figure 7. Left: energy difference ΔE for the ground-state energy (in CCSD approximation) of ^{24}O as a function of L_{eff} in a log plot. The symbols are as in Fig. 3, and the dashed line is the exponential fit for $N_{\text{max}} = 12$ from Table 3. Right: ground-state energies as a function of $\hbar\Omega$ as in the right panel of Fig. 3. The solid lines are fits of Eq. (6) for fixed N to only the solid points. The arrow marks the minimum energy $E_{\hbar\Omega \text{ min}}$ that is obtained when varying the oscillator spacing $\hbar\Omega$ for $N_{\text{max}} = 12$.

can be extrapolated from model spaces with $N = 8$.

We also tried to include $N = 6$ data points in the extrapolation, but the data points did not fall onto the same line as the $N = 8, 10, 12$ points. We speculate that this is due to peculiarities of the CCSD approximation, or due to a less complete decoupling of the center of mass in small model spaces [17]. Again, this points to the need to better understand the systematic errors involved in IR extrapolations of results obtained with approximate many-body results.

5. Summary

We studied IR extrapolations for coupled-cluster computations of oxygen isotopes with chiral nucleon-nucleon interactions at NNLO. One of the main results is the identification of the nucleus-dependent infrared box size L_{eff} . Our results show that IR extrapolations are feasible in practice, but we need a better understanding of systematic errors for extrapolated quantities; a Bayesian framework may be useful in this regard. Nevertheless, we demonstrated that reliable IR extrapolations can be performed in p - s - d nuclei spanning over tens of MeVs. For the IR extrapolations to work in practice one needs to minimize UV corrections and work at frequencies away from the usual range about the oscillator frequency that minimizes the energy at fixed number N of oscillator quanta.

Acknowledgments

This material is based upon work supported in part by the National Science Foundation under Grant No. PHY-1306250 (Ohio State University), by the U.S. Department of Energy, Office of Science, Office of Nuclear Physics, under Award Numbers DE-FG02-96ER40963 (University of Tennessee), DE-SC0008499/DE-SC0008533 (SciDAC-3 NUCLEI Collaboration), the Field Work Proposal ERKBP57 at Oak Ridge National Laboratory, and under contract number DEAC05-00OR22725 (Oak Ridge National Laboratory).

References

- [1] Navrátil P, Quaglioni S, Stetcu I and Barrett B R 2009 *Journal of Physics G: Nuclear and Particle Physics* **36** 083101 URL <http://stacks.iop.org/0954-3899/36/i=8/a=083101>
- [2] Barrett B R, Navrátil P and Vary J P 2013 *Progress in Particle and Nuclear Physics* **69** 131 – 181 URL <http://www.sciencedirect.com/science/article/pii/S0146641012001184>
- [3] Kümmel H, Lührmann K H and Zabolitzky J G 1978 *Physics Reports* **36** 1 – 63 URL <http://www.sciencedirect.com/science/article/pii/0370157378900819>
- [4] Bishop R F 1991 *Theoretical Chemistry Accounts: Theory, Computation, and Modeling (Theoretica Chimica Acta)* **80**(2) 95–148 10.1007/BF01119617 URL <http://dx.doi.org/10.1007/BF01119617>
- [5] Hagen G, Papenbrock T, Hjorth-Jensen M and Dean D J 2013 ArXiv:1312.7872 (*Preprint* 1312.7872) URL <http://adsabs.harvard.edu/abs/2013arXiv1312.7872H>

- [6] Dickhoff W and Barbieri C 2004 *Progress in Particle and Nuclear Physics* **52** 377 – 496 URL <http://www.sciencedirect.com/science/article/pii/S0146641004000535>
- [7] Tsukiyama K, Bogner S K and Schwenk A 2011 *Phys. Rev. Lett.* **106**(22) 222502 URL <http://link.aps.org/doi/10.1103/PhysRevLett.106.222502>
- [8] Hergert H, Binder S, Calci A, Langhammer J and Roth R 2013 *Phys. Rev. Lett.* **110**(24) 242501 URL <http://link.aps.org/doi/10.1103/PhysRevLett.110.242501>
- [9] Ekström A, Jansen G R, Wendt K A, Hagen G, Papenbrock T, Bacca S, Carlsson B and Gazit D 2014 ArXiv:1406.4696 URL <http://adsabs.harvard.edu/abs/2014arXiv1406.4696E>
- [10] Michel N, Nazarewicz W, Płoszajczak M and Vertse T 2009 *Journal of Physics G: Nuclear and Particle Physics* **36** 013101 URL <http://stacks.iop.org/0954-3899/36/i=1/a=013101>
- [11] Caprio M A, Maris P and Vary J P 2012 *Phys. Rev. C* **86**(3) 034312 URL <http://link.aps.org/doi/10.1103/PhysRevC.86.034312>
- [12] Bulgac A and Forbes M M 2013 *Phys. Rev. C* **87**(5) 051301 URL <http://link.aps.org/doi/10.1103/PhysRevC.87.051301>
- [13] Bogner S K, Kuo T T S and Schwenk A 2003 *Physics Reports* **386** 1 – 27 URL <http://www.sciencedirect.com/science/article/pii/S0370157303002953>
- [14] Bogner S K, Furnstahl R J and Perry R J 2007 *Phys. Rev. C* **75**(6) 061001 URL <http://link.aps.org/doi/10.1103/PhysRevC.75.061001>
- [15] Bohigas O, Tomsovic S and Ullmo D 1993 *Physics Reports* **223** 43 – 133 ISSN 0370-1573 URL [http://dx.doi.org/10.1016/0370-1573\(93\)90109-Q](http://dx.doi.org/10.1016/0370-1573(93)90109-Q)
- [16] Stetcu I, Barrett B and van Kolck U 2007 *Physics Letters B* **653** 358 – 362 URL <http://www.sciencedirect.com/science/article/pii/S0370269307009185>
- [17] Hagen G, Papenbrock T, Dean D J and Hjorth-Jensen M 2010 *Phys. Rev. C* **82**(3) 034330 URL <http://link.aps.org/doi/10.1103/PhysRevC.82.034330>
- [18] Coon S A, Avetian M I, Kruse M K G, van Kolck U, Maris P and Vary J P 2012 *Phys. Rev. C* **86**(5) 054002 URL <http://link.aps.org/doi/10.1103/PhysRevC.86.054002>
- [19] Furnstahl R J, Hagen G and Papenbrock T 2012 *Phys. Rev. C* **86**(3) 031301 URL <http://link.aps.org/doi/10.1103/PhysRevC.86.031301>
- [20] More S N, Ekström A, Furnstahl R J, Hagen G and Papenbrock T 2013 *Phys. Rev. C* **87**(4) 044326 URL <http://link.aps.org/doi/10.1103/PhysRevC.87.044326>
- [21] Furnstahl R J, More S N and Papenbrock T 2014 *Phys. Rev. C* **89**(4) 044301 URL <http://link.aps.org/doi/10.1103/PhysRevC.89.044301>
- [22] Jurgenson E D, Maris P, Furnstahl R J, Navrátil P, Ormand W E and Vary J P 2013 *Phys. Rev. C* **87**(5) 054312 URL <http://link.aps.org/doi/10.1103/PhysRevC.87.054312>
- [23] Roth R, Calci A, Langhammer J and Binder S 2013 ArXiv:1311.3563 URL <http://adsabs.harvard.edu/abs/2013arXiv1311.3563R>
- [24] Somà V, Barbieri C and Duguet T 2013 *Phys. Rev. C* **87**(1) 011303 URL <http://link.aps.org/doi/10.1103/PhysRevC.87.011303>
- [25] Hergert H, Bogner S K, Binder S, Calci A, Langhammer J, Roth R and Schwenk A 2013 *Phys. Rev. C* **87**(3) 034307 URL <http://link.aps.org/doi/10.1103/PhysRevC.87.034307>
- [26] Sääf D and Forssén C 2014 *Phys. Rev. C* **89**(1) 011303 URL <http://link.aps.org/doi/10.1103/PhysRevC.89.011303>
- [27] Olver F W J, Lozier D W, Boisvert R F and Clark C W (eds) 2010 *NIST Handbook of Mathematical Functions* (New York, NY: Cambridge University Press)
- [28] Bartlett R J and Musiał M 2007 *Rev. Mod. Phys.* **79**(1) 291–352 URL <http://link.aps.org/doi/10.1103/RevModPhys.79.291>
- [29] Hagen G, Papenbrock T, Dean D J and Hjorth-Jensen M 2008 *Phys. Rev. Lett.* **101**(9) 092502 URL <http://link.aps.org/doi/10.1103/PhysRevLett.101.092502>
- [30] Barbieri C and Hjorth-Jensen M 2009 *Phys. Rev. C* **79**(6) 064313 URL <http://link.aps.org/doi/10.1103/PhysRevC.79.064313>
- [31] Ekström A, Baardsen G, Forssén C, Hagen G, Hjorth-Jensen M, Jansen G R, Machleidt R,

- Nazarewicz W, Papenbrock T, Sarich J and Wild S M 2013 *Phys. Rev. Lett.* **110**(19) 192502
URL <http://link.aps.org/doi/10.1103/PhysRevLett.110.192502>
- [32] Dobaczewski J, Nazarewicz W and Reinhard P G 2014 *Journal of Physics G: Nuclear and Particle Physics* **41** 074001 URL <http://stacks.iop.org/0954-3899/41/i=7/a=074001>